

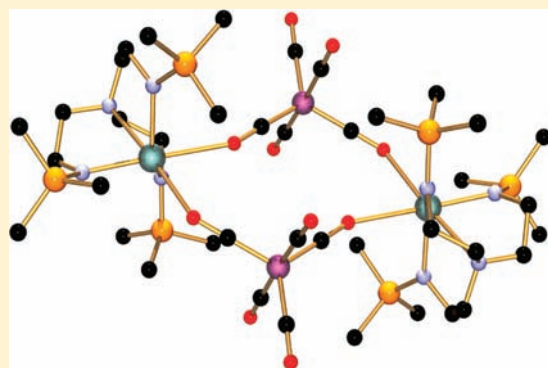
Halide, Amide, Cationic, Manganese Carbonylate, and Oxide Derivatives of Triamidosilylamine Uranium Complexes

Benedict M. Gardner, William Lewis, Alexander J. Blake, and Stephen T. Liddle*

School of Chemistry, University of Nottingham, University Park, Nottingham, NG7 2RD, United Kingdom

Supporting Information

ABSTRACT: Treatment of the complex $[\text{U}(\text{Tren}^{\text{TMS}})(\text{Cl})(\text{THF})]$ (**1**, $\text{Tren}^{\text{TMS}} = \text{N}(\text{CH}_2\text{CH}_2\text{NSiMe}_3)_3$) with Me_3SiI at room temperature afforded known crystalline $[\text{U}(\text{Tren}^{\text{TMS}})(\text{I})(\text{THF})]$ (**2**), which is reported as a new polymorph. Sublimation of **2** at 160°C and 10^{-6} mmHg afforded the solvent-free dimeric complex $[\{\text{U}(\text{Tren}^{\text{TMS}})(\mu\text{-I})\}_2]$ (**3**), which crystallizes in two polymorphic forms. During routine preparations of **1**, an additional complex identified as $[\text{U}(\text{Cl})_5(\text{THF})][\text{Li}(\text{THF})_4]$ (**4**) was isolated in very low yield due to the presence of a slight excess of $[\text{U}(\text{Cl})_4(\text{THF})_3]$ in one batch. Reaction of **1** with one equivalent of lithium dicyclohexylamide or bis(trimethylsilyl)amide gave the corresponding amide complexes $[\text{U}(\text{Tren}^{\text{TMS}})(\text{NR}_2)]$ (**5**, $R = \text{cyclohexyl}$; **6**, $R = \text{trimethylsilyl}$), which both afforded the cationic, separated ion pair complex $[\text{U}(\text{Tren}^{\text{TMS}})(\text{THF})_2][\text{BPh}_4]$ (**7**) following treatment of the respective amides with $\text{Et}_3\text{NH}\cdot\text{BPh}_4$. The analogous reaction of **5** with $\text{Et}_3\text{NH}\cdot\text{BAR}_f^f$ [$\text{Ar}^f = \text{C}_6\text{H}_3\text{-3,5-(CF}_3)_2$] afforded, following addition of **1** to give a crystallizable compound, the cationic, separated ion pair complex $[\{\text{U}(\text{Tren}^{\text{TMS}})(\text{THF})_2(\mu\text{-Cl})\}][\text{BAR}_f^f]$ (**8**). Reaction of **7** with $\text{K}[\text{Mn}(\text{CO})_5]$ or **5** or **6** with $[\text{HMn}(\text{CO})_5]$ in THF afforded $[\text{U}(\text{Tren}^{\text{TMS}})(\text{THF})(\mu\text{-OC})\text{Mn}(\text{CO})_4]$ (**9**); when these reactions were repeated in the presence of 1,2-dimethoxyethane (DME), the separated ion pair $[\text{U}(\text{Tren}^{\text{TMS}})(\text{DME})][\text{Mn}(\text{CO})_5]$ (**10**) was isolated instead. Reaction of **5** with $[\text{HMn}(\text{CO})_5]$ in toluene afforded $[\{\text{U}(\text{Tren}^{\text{TMS}})(\mu\text{-OC})_2\text{Mn}(\text{CO})_3\}_2]$ (**11**). Similarly, reaction of the cyclometalated complex $[\text{U}\{\text{N}(\text{CH}_2\text{CH}_2\text{NSiMe}_2\text{Bu}^t)_2(\text{CH}_2\text{CH}_2\text{NSiMe}_2\text{Bu}^t\text{CH}_2)\}_2]$ with $[\text{HMn}(\text{CO})_5]$ gave $[\{\text{U}(\text{Tren}^{\text{DMSB}})(\mu\text{-OC})_2\text{Mn}(\text{CO})_3\}_2]$ [**12**, $\text{Tren}^{\text{DMSB}} = \text{N}(\text{CH}_2\text{CH}_2\text{NSiMe}_2\text{Bu}^t)_3$]. Attempts to prepare the manganocene derivative $[\text{U}(\text{Tren}^{\text{TMS}})\text{MnCp}_2]$ from **7** and $\text{K}[\text{MnCp}_2]$ were unsuccessful and resulted in formation of $[\{\text{U}(\text{Tren}^{\text{TMS}})\}_2(\mu\text{-O})]$ (**13**) and $[\text{MnCp}_2]$. Complexes **3–13** have been characterized by X-ray crystallography, ^1H NMR spectroscopy, FTIR spectroscopy, Evans method magnetic moment, and CHN microanalyses.



INTRODUCTION

There is currently significant interest in the nonaqueous coordination and organometallic chemistry of uranium.^{1–11} This is motivated by the search for an improved understanding of the differences in covalent bonding between the 5f and 4f elements and for new reaction methodologies that might be applicable in catalytic reactions.¹² Although uranium complexes typically exhibit more covalent character in their bonding than analogous lanthanide complexes, it is necessary to precisely control the nature of the coordination sphere to tailor the properties and reactivity of the resultant complexes as electrostatic effects still dominate the bonding picture. Since uranium is a large metal (having a 1.70 Å single bond covalent radius according to Pyykkö)¹³ with many potential coordination sites, the use of multidentate ligands represents an effective strategy for controlling the number of reactive sites at uranium, as exemplified by the triamidoamine ligand $\{\text{N}(\text{CH}_2\text{CH}_2\text{NSiMe}_3)\}_3^{3-}$ (Tren^{TMS}), which has been utilized to great effect in recent years.^{14–26}

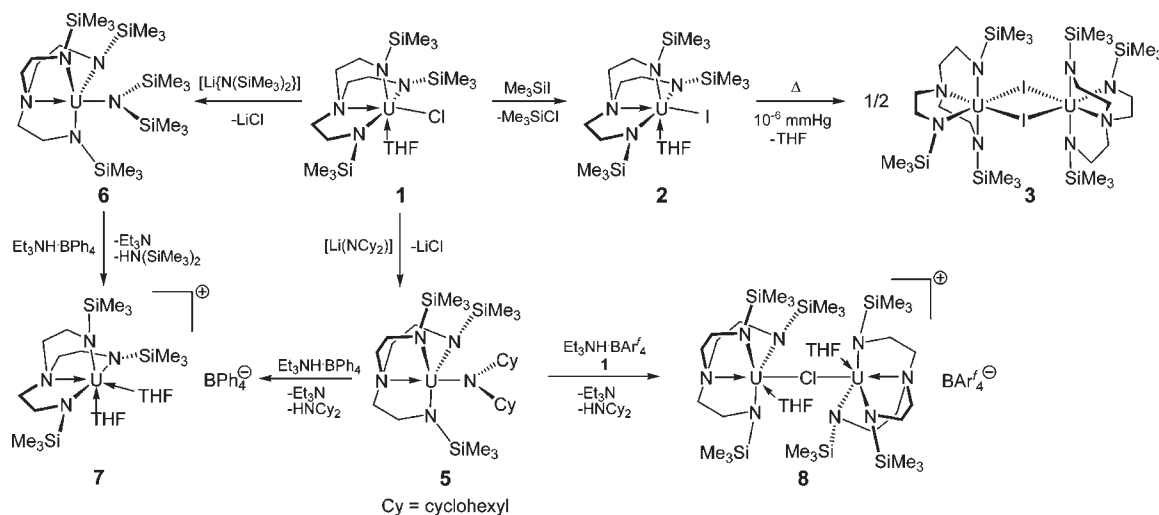
We recently embarked on a program of research to investigate the structure, bonding, and reactivity of complexes that contain uranium–metal bonds;^{27–34} this was stimulated by their paucity

in the literature compared to the well-developed area of metal–metal bonding in the d-block.^{6,7} We have found the Tren^{TMS} ligand to be an excellent ancillary ligand for complexes containing uranium–metal bonds, as demonstrated by our use of the complexes $[\text{U}(\text{Tren}^{\text{TMS}})(\text{X})(\text{THF})]$ ($\text{X} = \text{Cl}$, **1**; $\text{X} = \text{I}$, **2**)^{27,29} to prepare the first unsupported uranium–gallium²⁷ and uranium–rhenium²⁹ bonds, both of which are notable for containing σ - and π -components in the uranium(IV)–metal bonds, although the latter component is clearly weak. However, although **1** and **2** are in principle clearly good precursors for constructing uranium–metal bonds by salt elimination reactions, as evidenced by the aforementioned U–Ga and U–Re complexes, we have found that some transition metal anions, especially carbonylate anions, can exhibit sluggish reactivity that we ascribe to entrapment of the alkali metal counteraction by the carbonyl groups.³² This limitation can be overcome by thermolysis of reaction mixtures, but this could clearly lead to decomposition and is therefore undesirable.³⁰ However, amide and separated ion pair

Received: June 27, 2011

Published: August 31, 2011

Scheme 1. Synthesis of 2, 3, 5, 6, 7, and 8



derivatives of **1** and **2** represent valuable alternative precursors to uranium–metal bonds. The former would enable uranium–metal bonds to be constructed from a uranium amide and transition metal hydrides with concomitant elimination of amine.³⁵ The latter would provide the opportunity to conduct salt elimination chemistry under less forcing conditions than might be required with halide precursors, since the non/weakly coordinating anion of a separated ion pair should be easier to abstract and eliminate than a coordinated halide anion.³⁶ The use of uranium precursors free of coordinated Lewis bases such as ethers are potentially desirable, since the presence of ethers such as THF could provide a mechanism for decomposition by oxo-group abstraction.³⁷ Lastly, a library of Tren uranium precursor complexes is valuable in a broader synthetic context as a basis for new nonaqueous uranium chemistry.

Having successfully prepared U–Re bonds previously,²⁹ we investigated the possibility of preparing U–Mn bonds for comparative purposes and also with a view to determining their reactivity. Herein, we report the synthesis and characterization of a range of solvated and solvent-free uranium halide, amide, cationic, manganese carbonylate, and oxide complexes supported by Tren^{TMS} and the more sterically demanding variant Tren^{DMSB} [Tren^{DMSB} = N(CH₂CH₂NSiMe₂Bu^t)₃].

RESULTS AND DISCUSSION

Halide, Amide, and Cationic Derivatives. The triamidoamine uranium(IV) complex [U(Tren^{TMS})(Cl)(THF)] [**1**, Tren^{TMS} = {N(CH₂CH₂NSiMe₃)₃}³⁻] is readily prepared from [Li₃(Tren^{TMS})] and UCl₄ in THF and may be recrystallized in high yield as a THF adduct on a multigram scale.²⁷ Alternatively, **1** may be sublimed to give the solvent-free dimeric form.¹⁴ In common with related Tren and other uranium complexes,³⁸ complex **1** may be treated with Me₃SiI and converted to the corresponding iodide complex [U(Tren^{TMS})(I)(THF)] (**2**) in essentially quantitative yield,²⁹ with concomitant elimination of Me₃SiCl, and **2** can be recrystallized in excellent yields (Scheme 1). Although complete characterization of **2** has been reported by us previously,²⁹ during the course of routine crystallographic screening, we identified

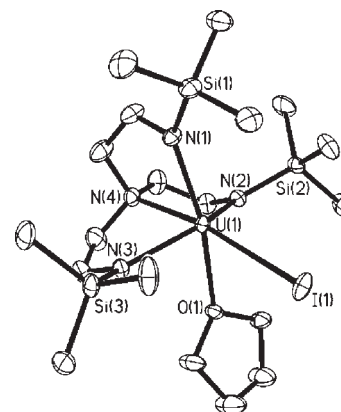


Figure 1. Molecular structure of **2** with selective atom labeling and probability ellipsoids set at 30%. Hydrogen atoms are omitted for clarity.

a new unit cell. Therefore, we carried out a full data collection to ascertain the identity of the apparently new compound that was subsequently found to be a polymorph of **2**.

The overall structure of **2** (Figure 1 and Table 1) is identical to the previously known polymorph in terms of connectivity; the uranium center adopts a distorted octahedral geometry, being coordinated by the four nitrogen centers of the quadridentate Tren ligand, an iodide which is *trans* to the datively bound amine center, and the oxygen donor of a THF molecule. The bond lengths and angles in **2** exhibit similar values to those in the previously reported polymorph, albeit with minor variations in the U–I, U–N, and U–O bond lengths, which are within literature ranges.³⁹

Realizing that an ether-free triamidoamine uranium(IV) iodide complex may prove to be a valuable and necessary precursor to uranium–metal bonds if ether cleavage/oxo-abstraction reactions occurred with ether-coordinated uranium precursors, we prepared [{U(Tren^{TMS})(μ-I)}₂] (**3**) quantitatively by sublimation of **2** at 160 °C and 10⁻⁶ mmHg. This afforded **3** as a pale yellow microcrystalline solid in quantitative yield (Scheme 1). The ¹H NMR spectrum of **3** spans the range +16 to –46 ppm, which compares to a range of +28 to –44 ppm for **2**.

Table 1. Selected Bond Lengths (Å) and Angles (deg) for **2**, **3**·**2C₇H₈**, and **3**·**0.5C₇H₈**

2			
U(1)–N(1)	2.283(8)	U(1)–N(2)	2.225(8)
U(1)–N(3)	2.250(7)	U(1)–N(4)	2.555(8)
U(1)–I(1)	3.1287(7)	U(1)–O(1)	2.558(6)
3 · 2C₇H₈			
U(1)–N(1)	2.234(3)	U(1)–N(2)	2.227(3)
U(1)–N(3)	2.224(2)	U(1)–N(4)	2.567(2)
U(1)–I(1)	3.2902(5)	U(1)–I(1A)	3.244(4)
U(1)–I(1AA)	3.1832(4)	U(1)–U(1B)	3.241(4)
3 · 0.5C₇H₈			
U(1)–I(1)	3.2246(5)	U(1)–I(1A)	3.261(6)
U(1)–I(1AA)	3.328(6)	U(1)–I(1B)	3.3768(5)
U(1)–N(1)	2.226(4)	U(1)–N(2)	2.246(5)
U(1)–N(3)	2.211(5)	U(1)–N(4)	2.570(4)
U(2)–I(2)	3.2095(5)	U(2)–I(2A)	3.229(8)
U(2)–I(2AA)	3.229(8)	U(2)–I(2B)	3.3354(5)
U(2)–N(5)	2.233(4)	U(2)–N(6)	2.228(4)
U(2)–N(7)	2.248(4)	U(2)–N(8)	2.570(4)

Table 2. Room Temperature Magnetic Moment Data for **1–3** and **5–13**^a

compound	aggregation	μ_B
1	m	2.78
2	m	2.79
3	d	3.88
5	m	2.79
6	m	3.03
7	m	2.10
8	d	3.51
9	m	2.94
10	m	3.35
11	d	3.93
12	d	4.09
13	d	2.95

^a m = monomeric; d = dimeric.

Spectroscopic and combustion analysis supported the proposed formulation, and the magnetic moment in solution at room temperature was found to be 3.88 μ_B (Table 2), which is consistent with a ³H₄ ground state of f² uranium(IV).⁴⁰

Complex **3** can be recrystallized in 80% yield as yellow-green needles from toluene solution, and an X-ray diffraction study was carried out to confirm the absence of coordinated THF (Figure 2 and Table 1). Two polymorphs of **3** were identified in the course of these studies. In one polymorph, half a dimer resides in the asymmetric unit and two molecules of toluene per dimer are found in the lattice. In the other polymorph, the asymmetric unit contains two half dimer molecules and half a molecule of toluene per dimer. The two polymorphs are denoted as **3**·**2C₇H₈** and **3**·**0.5C₇H₈**, and since they are generally similar with only minor variations in bond lengths and angles, we confine our discussion to one of the unique molecules in **3**·**0.5C₇H₈**. In **3**·**0.5C₇H₈**, which is a centrosymmetric dimer constructed around a four-

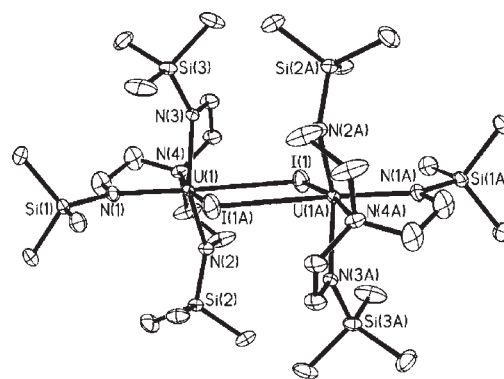
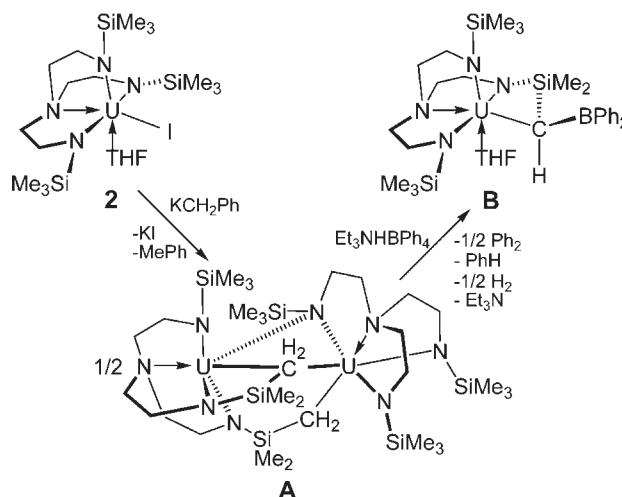


Figure 2. Molecular structure of **3**·**0.5C₇H₈** with selective atom labeling and probability ellipsoids set at 30%. Hydrogen atoms and minor iodide disorder components omitted for clarity. Only the major component of the disordered iodide and one of the two unique molecules are shown for clarity. The structure of **3**·**2C₇H₈** is very similar.

Scheme 2. Preparation of **A** and **B**^a



^a See ref 30 for full details.

membered U₂I₂ ring, each uranium adopts a distorted octahedral geometry defined by the four nitrogen centers of the Tren ligand and the two bridging iodides. The U–N_{amide} distances average 2.228(5) Å, which compares to averages of 2.252(3), 2.253(8), and 2.247(10) Å in **1**,²⁷ **2**,²⁹ and the solvent-free chloride analogue.¹⁴ Notably, the U(1)–N(2) bond length of 2.246(5) Å is longer than the U(1)–N(1) and U(1)–N(3) bond distances of 2.226(4) and 2.211(5) Å, perhaps reflecting the fact the former is *trans* to iodide whereas the latter pair are *cis* to iodide. The U(1)–N(4) bond length of 2.570(4) Å compares to a U–N_{amine} distance of 2.567(9) Å in [{U(Tren^{TMS})(μ-Cl)₂}]₂.¹⁴ The U–I bond distances fall within the literature range of U–I bond lengths but do not merit detailed discussion because of positional disorder of the iodide ligands in **3**·**2C₇H₈** and **3**·**0.5C₇H₈**.

On one occasion, we isolated a very small quantity (~2% yield) of pale green, almost colorless crystals from a preparation of **1**, which were subsequently identified as [U(Cl)₅(THF)][Li(THF)₄] (**4**), and this is deposited in the Supporting Information.

We have previously shown that **2** reacts with benzyl potassium to afford the tuck-in-tuck-over tuck-over dialkyl Tren

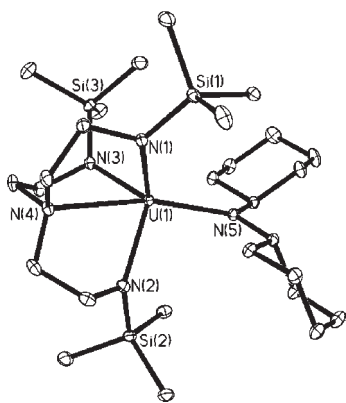


Figure 3. Molecular structure of **5** with selective atom labeling and probability ellipsoids set at 30%. Hydrogen atoms omitted for clarity.

complex $[U\{N(CH_2CH_2NSiMe_3)(CH_2CH_2NSiMe_2CH_2)_2\}-U(Tren^{TMS})]$ (**A**, Scheme 2),³⁰ and that treatment of **A** with $Et_3NH \cdot BPh_4$ affords the metallocyclic complex $[U\{N(CH_2CH_2NSiMe_3)_2(CH_2CH_2NSiMe_2C[H]BPh_2)\}(THF)]$ (**B**) rather than the anticipated ion pair complex $[(Tren^{TMS})U(THF)_n][BPh_4]$ (Scheme 2).³⁰ Since **A** and **B** have limited utility as precursors to uranium–metal bonds, we targeted amide derivatives. Amide derivatives would not be expected to generate cyclometalated species such as **A** from pK_a considerations as the corresponding reaction of **2** with benzyl potassium does. This would potentially enable the construction of uranium–metal bonds from a uranium amide and transition metal hydrides with concomitant elimination of amine.

Treatment of **1** with one equivalent of lithium dicyclohexylamide, or one equivalent of lithium bis(trimethylsilyl)amide, furnishes, after workup and recrystallization from hexane, yellow crystals of the complexes formulated as $[U(Tren^{TMS})(NR_2)]$ (**5**, $R = Cy = \text{cyclohexyl}$; **6**, $R = SiMe_3$) in 72% and 50% crystalline yield, respectively (Scheme 1). The 1H NMR spectra of **5** and **6** span the ranges +89 to –17 and +17 to –7 ppm, respectively, and together with the other spectroscopic and analytical data, support the proposed formulations. The solution magnetic moments of 2.79 and 3.03 μ_B for **5** and **6**, respectively, compare to moments of 2.78, 2.79, and 3.88 μ_B for **1**,²⁷ **2**,²⁹ and **3**, respectively, and are consistent with uranium(IV) centers (Table 2).

In **5** (Figure 3 and Table 3), the uranium center is 5-coordinate and can be considered to adopt a distorted trigonal bipyramidal geometry such that the N(4) and N(5) centers occupy the axial sites but the N(1), N(2), and N(3) centers are distorted from the equatorial plane by the constraints of the Tren ligand. The U(1)–N(1), U(1)–N(2), and U(1)–N(3) bond lengths of 2.289(2), 2.267(2), and 2.272(2) Å, respectively, are surprisingly longer overall than observed in **2**,²⁹ despite the 5-coordinate nature of the uranium center in **5** compared to the 6-coordinate uranium center in **2**. The U(1)–N(4) bond length of 2.696(2) Å is longer than the corresponding U–N bond distance of 2.555(8) Å in **2** reflecting the fact the former is *trans* to a dialkyl amide whereas the latter is *trans* to an iodide. The U(1)–N(5) bond length of 2.273(2) Å in **5** is shorter than the other U–N_{amide} distances as befits its dialkyl nature compared to the alkyl-silyl nature of the N(1)–N(3) centers. Interestingly, the U–NCy₂ bond length in **5** is longer than the U–NCy₂ bond distance of 2.210(3) Å in $[U(NCy_2)\{HC(SiMe_2NAr)_3\}(THF)]$ ($Ar = 3,5\text{-Me}_2\text{C}_6\text{H}_3$),³¹ which demonstrates the sterically demanding nature of Tren. The N(5) center adopts an essentially

Table 3. Selected Bond Lengths (Å) and Angles (deg) for **5**–**7**

		5		
U(1)–N(1)	2.289(2)		U(1)–N(2)	2.267(2)
U(1)–N(3)	2.272(2)		U(1)–N(4)	2.696(2)
U(1)–N(5)	2.273(2)			
		6		
U(1)–N(1)	2.247(6)		U(1)–N(2)	2.274(6)
U(1)–N(3)	2.245(6)		U(1)–N(4)	2.698(7)
U(1)–N(5)	2.329(6)			
		7·C₇H₈		
U(1)–N(1)	2.246(3)		U(1)–N(2)	2.243(3)
U(1)–N(3)	2.226(3)		U(1)–N(4)	2.542(3)
U(1)–O(1)	2.544(3)		U(1)–O(2)	2.592(3)

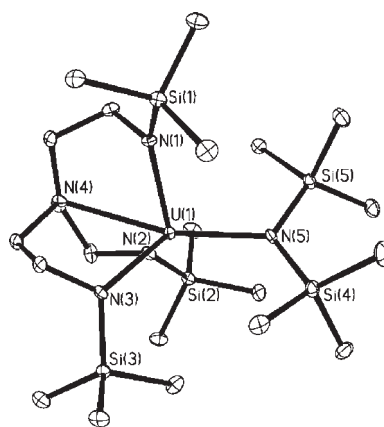


Figure 4. Molecular structure of **6** with selective atom labeling and probability ellipsoids set at 30%. Hydrogen atoms omitted for clarity.

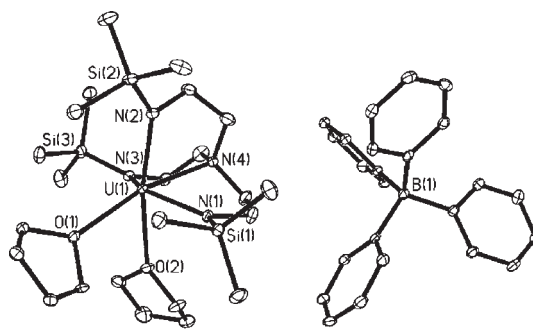
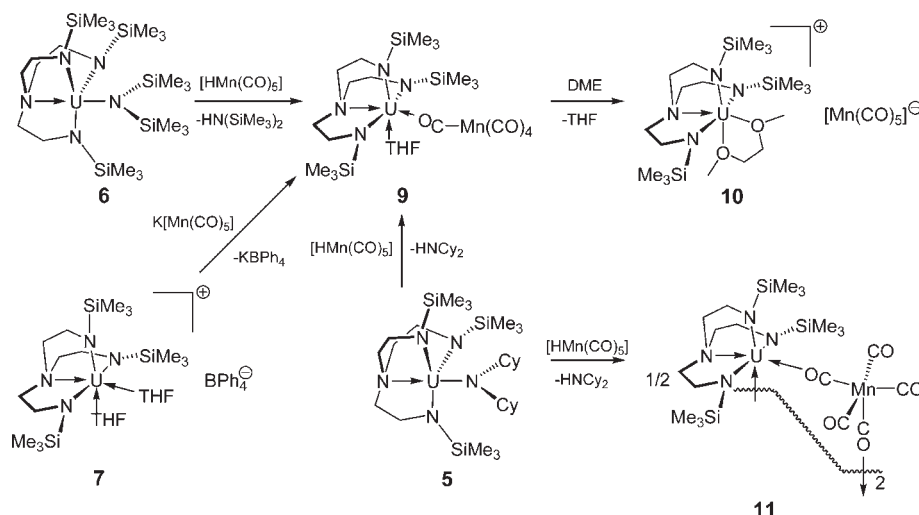


Figure 5. Molecular structure of **7·C₇H₈** with selective atom labeling and probability ellipsoids set at 30%. Hydrogen atoms and lattice toluene solvent omitted for clarity.

trigonal planar geometry [$\Sigma \angle = 359.97(17)^\circ$], which indicates that it is likely acting as a π -base to the electrophilic uranium center.

Analogously to **5**, complex **6** crystallizes with a 5-coordinate uranium center due to the sterically demanding ligands (Figure 4 and Table 3). The U(1)–N(1), U(1)–N(2), U(1)–N(3), and U(1)–N(4) bond lengths of 2.247(6), 2.274(6), 2.245(6), and 2.698(7) Å, respectively, compare well to **5**. The U(1)–N(5) bond distance of 2.329(6) Å is moderately longer than the other

Scheme 3. Synthesis of 9–11

Table 4. Comparison of Selected FTIR Data for Free CO, $K[Mn(CO)_5]$, $[HMn(CO)_5]$, and 9–12 in Nujol^a

compound	FTIR ν_{CO}/cm^{-1}
free CO	2143
$K[Mn(CO)_5]$	1835, 1909 ^a
$[HMn(CO)_5]$	1981, 2014 ^a
9	1709, 1889, 1918, 1931
10	1859, 1892, 1921, 1939
11	1731, 1814, 1823, 1938, 1952
12	1734 ^a , 1806 ^a , 1956 ^a

^a Broad band that obscures other absorptions in these regions.

three U–N_{amide} bond lengths, which reflects the presence of its silyl substituents. The N(5) center adopts an essentially trigonal planar geometry [$\Sigma\angle = 360.0(3)^\circ$], which indicates that it is likely acting as a π -base to the electrophilic uranium center.

With complexes 5 and 6 in hand, we explored their conversion to separated ion pair complexes. In light of the double-dearylation chemistry outlined in Scheme 2,³⁰ we tested the reactivity of 5 and 6 with $\text{Et}_3\text{NH} \cdot \text{BPh}_4$. Accordingly, treatment of 5 or 6 with $\text{Et}_3\text{NH} \cdot \text{BPh}_4$ in THF afforded, after work up, the separated ion pair complex $[\text{U}(\text{Tren}^{\text{TMS}})(\text{THF})_2][\text{BPh}_4^-]$ (7) as a free-flowing green powder from hexane in 95% yield (Scheme 1). The ^1H NMR spectrum of 7 exhibits resonances in the range +16 to –43 ppm, and the low solution magnetic moment of $2.10 \mu_{\text{B}}$ (Table 2) suggests that the orbital angular contribution at uranium may be suppressed, which may be due to the cationic nature of 7.⁴⁰ All other spectroscopic and analytical data support the proposed formulation. In order to assess whether complex 7 was a separated ion pair or a weakly associated contact ion pair, we conducted a single crystal X-ray diffraction experiment on a yellow-green crystal of $7 \cdot \text{C}_7\text{H}_8$ grown from toluene.

Complex 7 (Figure 5 and Table 3) crystallizes as a separated ion pair complex. The uranium center is coordinated to the four nitrogen centers of the Tren ligand and the oxygen centers of two molecules of THF in a distorted octahedral geometry with no contacts to the tetraphenylborate anion. The cationic nature of 7 is confirmed by inspection of the uranium–ligand bond lengths.

For example, the U(1)–N(1), U(1)–N(2), and U(1)–N(3) bond lengths of 2.246(3), 2.243(3), and 2.226(3) Å, respectively, give an average U–N_{amide} distance of 2.238(3) Å that compares to an average U–N_{amide} distance of 2.253(8) Å in 2.²⁹ The metrical parameters of the tetraphenylborate anion are unremarkable.

Since the tetraphenylborate anion is potentially not an innocent ligand and has precedent for mono-^{41–44} and double-dearylation³⁰ reactions in nonaqueous uranium chemistry, we investigated the use of the more robust borate anion BAr_4^- [$\text{Ar}^f = \text{C}_6\text{H}_3-3,5-(\text{CF}_3)_2$]⁴⁵ as an alternative non/weakly coordinating counteranion. Treatment of 5 with $\text{Et}_3\text{NH} \cdot \text{BAr}_4^-$ in THF affords, after work up, an oily yellow-brown product (Scheme 1). Although crude ^1H NMR spectra were consistent with the formation of the target complex $[\text{U}(\text{Tren}^{\text{TMS}})(\text{THF})_2][\text{BAr}_4^-]$, a number of intractable and unidentifiable impurities were observed that precluded the acquisition of further meaningful characterization data. In an effort to isolate a product cleanly, we added one equivalent of 1 to “ $[\text{U}(\text{Tren}^{\text{TMS}})(\text{THF})_2][\text{BAr}_4^-]$ ” in the anticipation that 1 would displace a coordinated THF molecule and bind via a bridging chloride to give an isolable complex. Accordingly, the cationic separated ion pair complex formulated as $[\{\text{U}(\text{Tren}^{\text{TMS}})(\text{THF})_2(\mu\text{-Cl})\}][\text{BAr}_4^-]$ (8) was isolated as pale green crystals, and full details can be found in the Supporting Information.

Carbonylate Derivatives. With the synthesis of 5–7 accomplished, we examined their reactivity toward the manganese pentacarbonyl anion in an attempt to prepare uranium–manganese bonds. Treatment of either 7 with $K[Mn(CO)_5]^{46}$ or 5 or 6 with $[HMn(CO)_5]^{47}$ resulted in elimination of KBPh_4 or HNCy_2 and $\text{HN}(\text{SiMe}_3)_2$, respectively, to afford the complex formulated as $[\text{U}(\text{Tren}^{\text{TMS}})(\text{THF})(\mu\text{-OC})\text{Mn}(\text{CO})_4]$ (9) (Scheme 3). Complex 9 was isolated as yellow blocks in 54% crystalline yield. Complex 9 could also be prepared by reaction of 2 with $K[Mn(CO)_5]$, but this required extended thermolysis and isolated yields were much lower ($\sim 15\%$), which demonstrates the utility of 7. The ^1H NMR spectrum covers the range +34 to –43 ppm, and the solution magnetic moment of 9 of $2.94 \mu_{\text{B}}$ (Table 2) is comparable to those of 1 and 2. The FTIR spectrum of 9 exhibits four strong carbonyl stretches at 1709, 1889, 1918, and

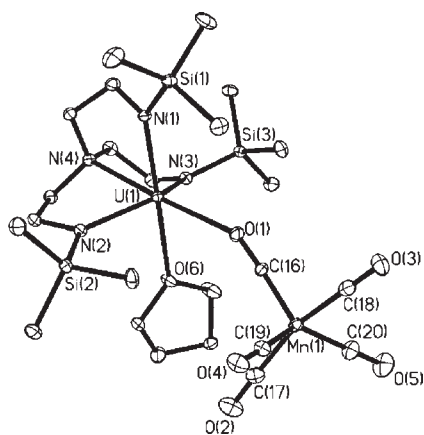


Figure 6. Molecular structure of **9** with selective atom labeling and probability ellipsoids set at 30%. Hydrogen atoms omitted for clarity.

1931 cm^{-1} that are consistent with substantial redistribution of the anionic charge of the manganese pentacarbonyl fragment to the carbonyl groups by manganese–carbonyl backbonding (Table 4). Based on a comparison with **10–12**, we tentatively assign the stretch at 1709 cm^{-1} to the isocarbonyl group. The presence of four carbonyl stretches in the FTIR spectrum of **9** is consistent with the approximate C_{2v} symmetry of the coordinated $\text{Mn}(\text{CO})_5^-$ anion in the solid state structure of **9** (vide infra).

The crystal structure of complex **9** confirms the presence of a bridging isocarbonyl CO ligand between the uranium and manganese centers (Figure 6 and Table 5), and this is reminiscent of $[\text{Yb}(\text{Cp}^*)_2(\text{THF})(\mu\text{-OC})\text{Co}(\text{CO})_3]$.⁴⁸ The coordination geometry around uranium is best described as distorted octahedral, with the Tren^{TMS} ligand coordinating facially, occupying four coordination sites. O(1) resides essentially *trans* to the amine nitrogen N(4), and a molecule of THF completes the coordination sphere. The geometry of the Tren^{TMS} ligand is unexceptional, with the $\text{U}-\text{N}_{\text{amide}}$ and $\text{U}-\text{N}_{\text{amine}}$ bond lengths of 2.231(3) (av.) and 2.570(3) Å, respectively, being in line with the Tren compounds described above. The $\text{U}(1)-\text{O}(1)$ and $\text{U}(1)-\text{O}(6)$ bond lengths of 2.496(3) and 2.512(2) Å, respectively, are also unexceptional. The Mn(1) atom adopts a slightly distorted square pyramidal geometry, with Mn–C and C–O bond lengths lying within the range of those in previously reported complexes.³⁹ The formation of an isocarbonyl linkage rather than a U–Mn bond highlights the oxophilicity of uranium but also contrasts with the complex $[(\text{Bu}^t\text{O})_3\text{TiMn}(\text{CO})_5]$ that contains a highly oxophilic titanium center but still forms a Ti–Mn bond.⁴⁹ Given that three Bu^tO groups at titanium can be considered to present a fairly sterically congested coordination environment, this suggests that the absence of a U–Mn bond in **9** might be attributed to the likely poor orbital overlap between 3d Mn and 5f/6d U rather than to steric factors, although the latter could play a significant role. Of course, the nature of the solvent could also affect the likelihood of U–Mn bond formation. However, reactions were found to be sluggish in hydrocarbon solvents. We therefore tried 1,2-dimethoxyethane (DME) solvent.

Repeating reactions of **7** with $\text{K}[\text{Mn}(\text{CO})_5]$ in DME or **5** or **6** with $[\text{HMn}(\text{CO})_5]$ or adding DME to **9** resulted in formation of the separated ion pair complex $[\text{U}(\text{Tren}^{\text{TMS}})(\text{DME})]-[\text{Mn}(\text{CO})_5]$ (**10**, Scheme 3). Complex **10** was isolated in 24% crystalline yield as yellow blocks. The ^1H NMR spectrum of **10**

Table 5. Selected Bond Lengths (Å) and Angles (deg) for **9–12**

9			
U(1)–N(1)	2.235(3)	U(1)–N(2)	2.234(3)
U(1)–N(3)	2.225(3)	U(1)–N(4)	2.570(3)
U(1)–O(6)	2.512(2)	U(1)–O(1)	2.496(3)
Mn(1)–C(16)	1.759(4)	Mn(1)–C(17)	1.830(5)
Mn(1)–C(18)	1.836(5)	Mn(1)–C(19)	1.824(4)
Mn(1)–C(20)	1.824(5)	C(16)–O(1)	1.182(4)
C(17)–O(2)	1.152(5)	C(18)–O(3)	1.140(5)
C(19)–O(4)	1.135(4)	C(20)–O(5)	1.154(5)
10			
U(1)–N(1)	2.219(2)	U(1)–N(2)	2.236(2)
U(1)–N(3)	2.222(2)	U(1)–N(4)	2.603(2)
U(1)–O(1)	2.539(2)	U(1)–O(2)	2.545(2)
Mn(1)–C(20)	1.824(3)	Mn(1)–C(21)	1.820(3)
Mn(1)–C(22)	1.808(2)	Mn(1)–C(23)	1.802(2)
Mn(1)–C(24)	1.808(3)	C(20)–O(3)	1.153(3)
C(21)–O(4)	1.150(3)	C(22)–O(5)	1.156(3)
C(23)–O(6)	1.161(3)	C(24)–O(7)	1.154(3)
11			
U(1)–N(1)	2.201(3)	U(1)–N(2)	2.211(3)
U(1)–N(3)	2.221(3)	U(1)–N(4)	2.631(3)
U(1)–O(1)	2.640(2)	U(1)–O(4A)	2.534(2)
Mn(1)–C(16)	1.788(3)	Mn(1)–C(17)	1.837(4)
Mn(1)–C(18)	1.838(4)	Mn(1)–C(19)	1.762(3)
Mn(1)–C(20)	1.825(4)	C(16)–O(1)	1.175(4)
C(17)–O(2)	1.146(4)	C(18)–O(3)	1.144(4)
C(19)–O(4)	1.192(4)	C(20)–O(5)	1.160(4)
12			
U(1)–N(1)	2.212(9)	U(1)–N(2)	2.204(9)
U(1)–N(3)	2.227(9)	U(1)–N(4)	2.599(9)
U(1)–O(1)	2.479(8)	U(1)–O(4A)	2.705(8)
Mn(1)–C(25)	1.752(11)	Mn(1)–C(26)	1.833(11)
Mn(1)–C(27)	1.846(12)	Mn(1)–C(28)	1.781(11)
Mn(1)–C(29)	1.853(13)	C(25)–O(1)	1.193(13)
C(26)–O(2)	1.159(14)	C(27)–O(3)	1.124(14)
C(28)–O(4)	1.165(13)	C(29)–O(5)	1.143(15)

spans the range +19 to –47 ppm, which is diagnostic of its conversion from **9**. The solution magnetic moment of **10** was found to be 3.35 μ_{B} (Table 2), which is surprisingly high compared to cationic **7**, which underscores the complexity of uranium orbital magnetism. The free $\text{Mn}(\text{CO})_5^-$ has D_{3h} symmetry and should only exhibit two FTIR active bands according to Group Theory considerations. However, the FTIR spectrum of **10** contains four carbonyl stretching bands at 1859, 1892, 1921, and 1939 cm^{-1} (Table 4). This phenomena most likely arises from solid-state effects whereby the local symmetry at manganese is lowered from D_{3h} , for example, to C_{2v} , which facilitates the emergence of more FTIR active bands. This postulate is supported by the crystal structure of **10** (vide infra).

Complex **10** (Figure 7 and Table 5) crystallizes as a separated ion pair complex. The uranium center is 6-coordinate and adopts a distorted octahedral geometry due to the bite angle of the DME ligand [63.94(5)°]. The coordinated molecule of DME occupies two coordination sites at uranium, with O(2) residing axially,

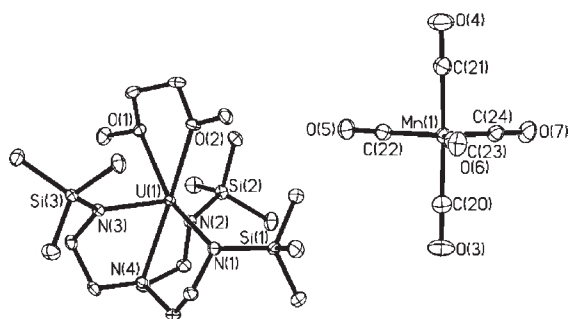


Figure 7. Molecular structure of **10** with selective atom labeling and probability ellipsoids set at 30%. Hydrogen atoms omitted for clarity.

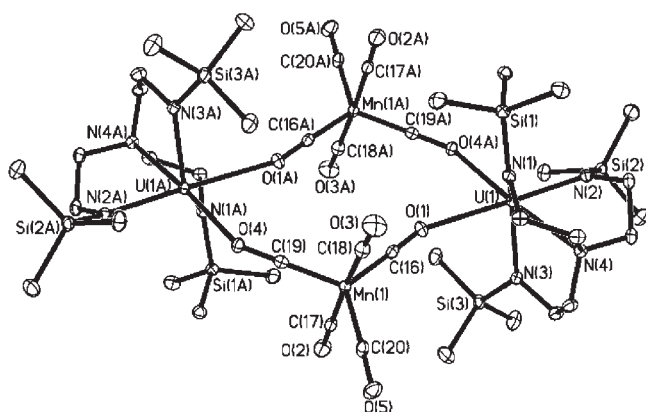
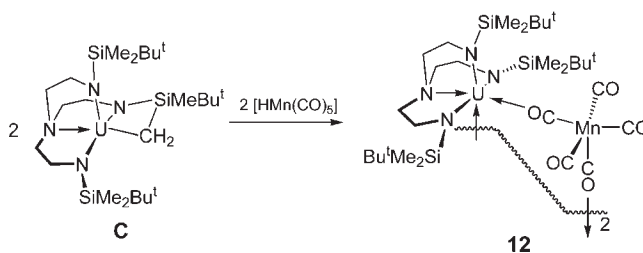


Figure 8. Molecular structure of **11** with selective atom labeling and probability ellipsoids set at 30%. Hydrogen atoms omitted for clarity.

essentially *trans* to the amine nitrogen N(4) and O(1) in an equatorial location. The geometry of the Tren^{TMS} ligand is unexceptional, and the U–N_{amide} and U–N_{amine} bond lengths of 2.2255(18) (av) and 2.6031(17) Å, respectively, are relatively short and compare well to the corresponding values in cationic **7**. The U(1)–O(1) and U(1)–O(2) bond lengths of 2.5388(14) and 2.5454(14) Å, respectively, are unexceptional. The manganese center adopts a distorted, axially elongated, trigonal bipyramidal geometry as evidenced by equatorial Mn(1)–C(22), Mn(1)–C(23), and Mn(1)–C(24) distances of 1.808(2), 1.802(2), and 1.808(3) Å, respectively, and longer axial Mn(1)–C(20) and Mn(1)–C(21) bond lengths of 1.824(3) and 1.820(3) Å, respectively. This axial elongation is rationalized by simple crystal field considerations and is consistent with the observed FTIR spectrum for **10**.

Reasoning that donor solvent might be precluding formation of a U–Mn bond, as found in **10**, we examined the reaction between solvent free **5** and **6** with [HMn(CO)₅] in nondonor solvent. Accordingly, yellow [$\{U(\text{Tren}^{\text{TMS}})(\mu\text{-OC})_2\text{Mn}(\text{CO})_3\}_2$] (**11**) was isolated in 73% crystalline yield (Scheme 3). Despite the dimeric formulation determined in the solid state (vide infra), the ¹H NMR spectrum contains only three resonances spanning the range +20 to –45 ppm. Variable temperature NMR was not investigated due to the low solubility of **11** in arene solvents, and the addition of THF afforded **9**. The solution magnetic moment of dimeric **11** is 3.93 μ_B (Table 2). The FTIR spectrum of **11** exhibits five carbonyl bands at 1731, 1814, 1823, 1938, and 1952 cm^{–1} (Table 4), which reflects the relatively low symmetry at manganese and the presence of two bridging

Scheme 4. Synthesis of **12**



carbonyl groups in the solid state (vide infra). In common with **9**, we tentatively assign the carbonyl stretch at 1731 cm^{–1} to an isocarbonyl group.

Complex **11** crystallizes as a centrosymmetric, THF free, dimer with distorted octahedral uranium centers (Figure 8 and Table 5) and is reminiscent of [Yb(Cp^{*})₂(μ-OC)₂Mn(CO)₃]₂.⁵⁰ The U–N_{amide} bond distances span the range 2.201(3)–2.221(3) Å. These distances can be considered relatively short, perhaps reflecting that the coordination sphere of each uranium center is completed by two oxygen atoms from isocarbonyl groups that must be considered as weakly bound considering DME and THF are capable of displacing them. The U(1)–O(1) and U(1)–O(4) bond lengths are 2.640(2) and 2.534(2) Å, respectively, which reflects the fact the former is *trans* to an anionic amide whereas the latter resides *trans* to a neutral, dative amine center. This is reflected in the Mn–C bond lengths. For example, the longer U(1)–O(1) bond compared to the U(1)–O(4) suggests there is less formal negative charge on O(1) compared to O(4), which implies that the backbonding from manganese to carbon is less. Therefore, the Mn(1)–C(16) bond length [1.788(3) Å] should be longer than the Mn(1)–C(19) distance [1.762(3) Å], which is indeed the case. Furthermore, increased backbonding from manganese to carbon as a consequence of charge polarization toward the electropositive uranium center is evidenced by longer Mn(1)–C(17), Mn(1)–C(18), and Mn(1)–C(20) bond lengths of 1.837(4), 1.838(4), and 1.825(4) Å compared to the Mn(1)–C(16) and Mn(1)–C(19) distances. Within the latter three Mn–C bonds, the axial pair [C(17) and C(18)] appear to be elongated compared to C(20) as observed in **10**. Lastly, the expected lengthening of the O–C_{carbonyl} bond distances in the bridging isocarbonyls, as a result of increased Mn–C backbonding, is evident in **11**. For example, the isocarbonyl C(16)–O(1) and C(19)–O(4) bond lengths are 1.175(4) and 1.192(4) Å, respectively, and are longer than the terminal C(17)–O(2), C(18)–O(3), and C(20)–O(5) bond distances of 1.146(4), 1.144(4), and 1.160(4) Å, respectively.

For completeness, we investigated the reaction of the known cyclometalated, tuck-in complex [U{N(CH₂CH₂NSiMe₂Bu^t)₂–(CH₂CH₂NSiMeBu^tCH₂)₂}] (**C**),²⁰ with [HMn(CO)₅] in toluene. Accordingly, yellow-green crystals of [$\{U(\text{Tren}^{\text{DMSB}})(\mu\text{-OC})_2\text{Mn}(\text{CO})_3\}_2$] [**12**, Tren^{DMSB} = N(CH₂CH₂NSiMe₂Bu^t)₃] were isolated in 60% yield (Scheme 4). Thus, formal salt, amine, and alkane elimination methods provide access to uranium manganese carbonylate complexes. Like **11**, the ¹H NMR spectrum of **12** is relatively simple and exhibits four resonances over the range +16 to –38 ppm despite the dimeric formulation in the solid state, and variable temperature NMR experiments were not practicable due to the poor solubility of **12** in arene solvents.

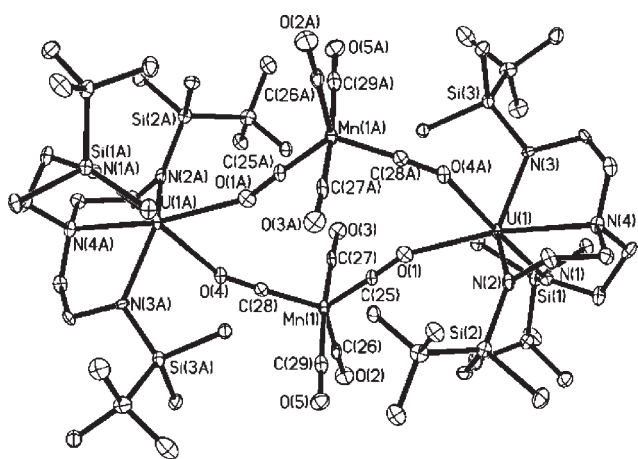
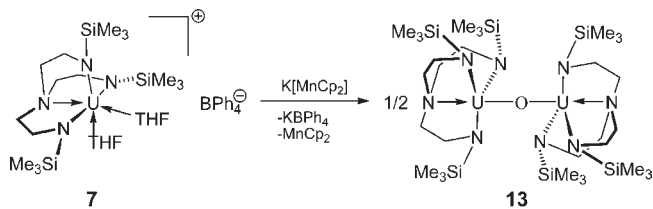


Figure 9. Molecular structure of **12** with selective atom labeling and probability ellipsoids set at 30%. Hydrogen atoms omitted for clarity.

Scheme 5. Synthesis of **13**



The solution magnetic moment of **12** was found to be $4.09 \mu_B$ (Table 2), which is comparable to that of **11**. The FTIR spectrum of **12** contains only three clear-cut carbonyl absorptions at 1734, 1806, and 1956 cm^{-1} (Table 4), compared to five absorptions for **11**, but these bands are broad and clearly obscure other absorptions in this region. The isocarbonyl stretching band at 1734 cm^{-1} for **12**, assigned on the basis of **9** and **11**, is shifted only 3 cm^{-1} from the corresponding band in **11**.

The structure of **12** (Figure 9 and Table 5) is very similar to that of **11**. Indeed, regarding the manganese pentacarbonyl fragment, exactly the same trends are observed regarding the Mn–C and C–O bond lengths. Specifically, the isocarbonyl groups exhibit shorter Mn–C bonds and longer C–O bonds compared to the terminal carbonyl groups, as a result of increased backbonding to facilitate charge polarization toward the electrophilic uranium centers, and within the latter group, the axial carbonyls show elongated Mn–C bonds compared to the equatorial carbonyl.

Oxo Derivative. The formation of **9–12** suggested that the formation of uranium–manganese bonds is unlikely to occur in the presence of carbonyl groups due to isocarbonyl bonding being favored for oxophilic uranium(IV). Since we have had significant success with the rhenocene fragment, we investigated the use of manganocene, since the 18-electron potassium complex $\text{K}[\text{MnCp}_2]$ ⁵¹ is known. However, we did not investigate the potential use of $[\text{HMnCp}_2]$ due to its unstable nature.⁵² Although $\text{K}[\text{MnCp}_2]$ is accessible, it is also relatively unstable and easily decomposes to the 17-electron parent manganocene. Therefore, we selected complex **7** for this reaction because we surmised that any sluggish reactivity could not be countered with thermolysis due to the instability of $\text{K}[\text{MnCp}_2]$. However,

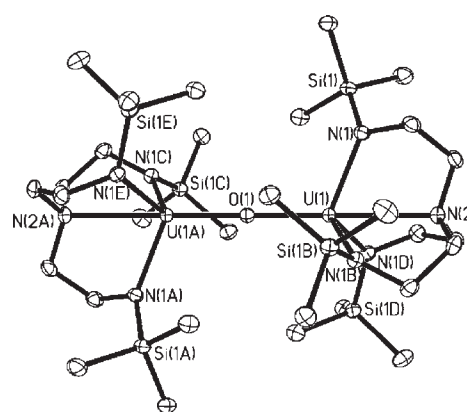


Figure 10. Molecular structure of **13** with selective atom labeling and probability ellipsoids set at 30%. Hydrogen atoms omitted for clarity.

although the reaction of **7** with $\text{K}[\text{MnCp}_2]$ proceeds under a variety of reaction conditions with elimination of potassium tetraphenylborate, significant quantities of manganocene were isolated from reaction mixtures, and fractional crystallization afforded the oxo complex $[\{\text{U}(\text{Tren}^{\text{TMS}})\}_2(\mu\text{-O})]$ (**13**) as yellow plates in 82% isolated yield (Scheme 5). The oxo-group abstraction most likely originates from the coordinated THF solvent in **7**,⁵³ and we propose that, following salt elimination, a putative $[\text{U}(\text{Tren}^{\text{TMS}})\text{MnCp}_2]$ complex is formed but homolytic bond cleavage occurs to yield 17 valence electron manganocene and $[\text{U}(\text{Tren}^{\text{TMS}})]$. This would necessarily require inner-sphere electron transfer, but we also cannot rule out an outer-sphere electron transfer mechanism. The latter complex would be highly reactive by virtue of its uranium(III) formulation, resulting in oxo-abstraction and favorable oxidation of uranium from a III to IV state.

The identity of **13** was confirmed by X-ray diffraction (Figure 10). Complex **13** crystallizes with N(2)–U(1)–O(1) aligned along a crystallographic 3-fold axis, and O(1) resides on an inversion center. The U(1)–N(1) and U(1)–O(1) bond lengths of 2.263(2) and 2.13197(19) Å, are unremarkable and consistent with the uranium(IV) formulation of **13**.

SUMMARY AND CONCLUSIONS

To summarize, we have reported a series of halide, amide, and cationic separated ion pair derivatives of a triamidoamine uranium complex that represent valuable precursors for nonaqueous uranium chemistry. Whereas the use of alkyl derivatives gives cyclometalation chemistry and fragmentation of tetraphenylborate anion, the corresponding amide derivatives yield the anticipated separated ion pair derivatives in a straightforward manner. The potential utility of the halide, amide, and cationic complexes is demonstrated by the synthesis of a range of manganese carbonylate complexes. No uranium–manganese bonds were formed, and instead, isocarbonyl linkages dominate in the products formed from a variety of routes and precursors. Therefore, we conclude that, in these Tren systems, the valence orbital on manganese is possibly too contracted to make bonding with oxophilic 5f/6d uranium(IV) favorable when isocarbonyl linkages are available. Additionally, sterics are likely to play a role in the preferential formation of isocarbonyl linkages. Attempts to prepare a uranium–manganese bond with the manganocene anion were unsuccessful, which possibly suggests that the formation of such linkages is inherently unfavorable. We are

currently investigating the reactivity of **9**–**12** and will report on this work in due course.

EXPERIMENTAL SECTION

General. All manipulations were carried out using standard Schlenk techniques, or an MBraun UniLab glovebox, under an atmosphere of dry nitrogen. Solvents were dried by passage through activated alumina towers and degassed before use. All solvents were stored over potassium mirrors, with the exception of THF and DME, which were stored over activated 4 Å molecular sieves. Deuterated solvents were distilled from potassium, degassed by three freeze–pump–thaw cycles and stored under nitrogen. Compounds **1**,²⁷ **2**,²⁸ **C**,²⁰ [Li(NC₂Y₂)],³¹ Et₃NH·BPh₄,⁵⁴ Et₃NH·BAR_f⁴⁵ K[Mn(CO)₅],⁴⁶ [HMn(CO)₅],⁴⁷ and K[MnCP₂]⁵¹ were prepared according to published procedures.

¹H NMR spectra were recorded on a Bruker 400 spectrometer operating at 400.2 MHz; chemical shifts are quoted in parts per million and are relative to TMS. FTIR spectra were recorded on a Bruker Tensor 27 spectrometer. Elemental microanalyses were carried out by Medac Ltd., U.K. The very small yield of **4** precluded any analysis other than its crystal structure. Satisfactory CHN data could not be obtained for **10**; the ¹H NMR spectrum of **10** is therefore included in the Supporting Information (Figure S3).

Preparation of [U(Tren^{TMS})(μ-I)]₂ (3**).** Compound **2** (3.16 g, 3.97 mmol) was sublimed at 160 °C at 10^{−6} mmHg for 8 h to yield a yellow crystalline solid in quantitative yield. This was dissolved in hot (70 °C) toluene (5.0 mL), filtered while hot, and then stored at −30 °C for 72 h to yield yellow-green crystals of **3** (3·0.5C₇H₈ and 3·2C₇H₈ from different batches) suitable for single-crystal X-ray crystallography. Yield: 2.59 g, 80%. Anal. Calcd for C₃₀H₇₈I₂N₈Si₆U₂: C, 24.86; H, 5.42; N, 7.73%. Found: C, 24.21; H, 5.36; N, 6.93%. ¹H NMR: (C₆D₆, 298 K) δ −45.17 (s, 12H, CH₂), 12.35 (s, 54H, SiMe₃), 15.19 (s, 12H CH₂). FTIR ν/cm^{−1} (Nujol): 1726 (w), 1260 (m), 1248 (m), 1141 (m), 1083 (m), 1053 (m), 927 (m), 896 (m), 839 (s), 800 (m), 743 (w), 723 (w), 678 (m), 623 (m). μ_{eff} (Evans method, 298 K): 3.88 μ_B.

Preparation of [U(Tren^{TMS})(NCy₂)] (5**).** Toluene (30 mL) was added to a cold (−78 °C) mixture of **1** (0.71 g, 1.00 mmol) and lithium dicyclohexylamide (0.19 g, 1.00 mmol). The resulting suspension was allowed to warm to ambient temperature while being stirred over 1 h, before being stirred at ambient temperature for a further 16 h. Volatiles were removed in vacuo from the yellow-brown turbid reaction mixture to yield a brown solid. Hexane (20 mL) was added, and the resulting suspension was allowed to settle. The brown solution was filtered away from the off-white precipitate, before the solvent was reduced in volume to 10 mL in vacuo and stored at −80 °C for 18 h to yield yellow crystals of **5** suitable for single-crystal X-ray crystallography. Yield: 0.56 g, 78%. Anal. Calcd for C₃₅H₆₁N₅Si₃U: C, 41.68; H, 7.90; N, 9.00%. Found: C, 40.87; H, 8.49; N, 9.21%. ¹H NMR: (C₆D₆, 298 K) δ −16.07 (s, 27H, SiMe₃), −6.10 (s, 6H, CH₂), 5.86 (4H, s, Cy−CH₂), 5.98 (s, 4H, Cy−CH₂), 7.87 (s, 4H, Cy−CH₂), 12.03 (s, 4H, Cy−CH₂), 14.36 (s, 4H, Cy−CH₂), 36.17 (s, 6H, CH₂), 88.07 (s, 2H, CH). FTIR ν/cm^{−1} (Nujol): 1590 (w), 1258 (m), 1244 (m), 1142 (w), 1110 (w), 1067 (m), 1025 (m), 926 (m), 899 (w), 835 (s), 770 (m), 742 (m), 722 (m), 693 (m), 677 (w). μ_{eff} (Evans method, 298 K): 2.79 μ_B.

Preparation of [U(Tren^{TMS}){N(SiMe₃)₂}] (6**).** THF (20 mL) was added to a cold (−78 °C) mixture of **2** (1.59 g, 2.0 mmol) and [KN(SiMe₃)₂] (0.40 g, 2.0 mmol). The resulting suspension was allowed to warm to ambient temperature while being stirred (1 h), before being stirred at ambient temperature for a further 16 h. The dark yellow turbid reaction mixture was filtered, and volatiles were removed in vacuo to yield a pale yellow solid. Hexane (15 mL) was added, and the resulting suspension was allowed to settle and was filtered. The dark yellow solution was reduced in volume to 3 mL in vacuo and stored at −30 °C for 18 h to yield yellow crystals, which were collected at −30 °C

by filtration and washed with cold pentane (2 × 2 mL). Yield: 0.76 g, 50%. Anal. Calcd for C₂₁H₅₇N₅Si₃U: C, 33.27; H, 7.58; N, 9.24%. Found: C, 33.18; H, 7.53; N, 9.39%. ¹H NMR: (C₆D₆, 298 K) δ −6.88 (s, 18H, {N(SiMe₃)₂}), −3.85 (s, 27H, SiMe₃), −1.83 (6H, s, CH₂), 17.08 (s, 6H, CH₂). FTIR ν/cm^{−1} (Nujol): 1725 (w), 1658 (w), 1258 (s), 1246 (s), 1180 (w), 1146 (m), 1137 (m), 1056 (s), 1028 (m), 1018 (m), 933 (vs), 898 (m), 838 (vs), 773 (s), 740 (m), 723 (m), 672 (m), 609 (m), 588 (w), 566 (w), 550 (w), 522 (w), 465 (w), 437 (m). μ_{eff} (Evans method, d₈-THF, 298 K): 3.03 μ_B.

Preparation of [U(Tren^{TMS})(THF)₂][BPh₄] (7**).** THF (40 mL) was added to a cold (−78 °C) mixture of **5** (1.94 g, 2.50 mmol) and Et₃NH·BPh₄ (1.05 g, 2.50 mmol). The resulting suspension was allowed to warm to ambient temperature while being stirred over 1 h, before being stirred at ambient temperature for a further 16 h. Volatiles were removed in vacuo to yield a yellow-green oil. Toluene (50 mL) was added and gently warmed to 60 °C while stirring, before being allowed cool to ambient temperature to yield a yellow-brown solution and green oil. The solution was decanted from the oil, reduced to 25 mL in vacuo and was stored at ambient temperature for 21 days to yield a small crop of yellow-green crystals of 7·C₇H₈ suitable for single-crystal X-ray crystallography. Alternatively, the oil was vigorously stirred in 80 mL of hexane for 7 days to yield a pale green free-flowing precipitate. Yield: 0.29 g, 10% (crystalline); 2.73 g, 95% (powder). The synthesis of **7** from **6** is analogous. Anal. Calcd for C₄₇H₇₅BN₄O₂Si₃U: C, 53.19; H, 7.12; N, 5.28%. Found: C, 52.90; H, 6.78; N, 5.35%. ¹H NMR: (d₈-THF, 298 K) δ −42.90 (s, 6H, CH₂), −0.07 (m, 12H, Ar−H), 1.77 (m, 8H, Ar−H), 3.84 (s, 8H, THF), 4.10 (s, 8H, THF), 7.53 (s, 27H, SiMe₃), 15.54 (s, 6H, CH₂). ¹¹B NMR: (d₈-THF, 298 K) δ −10.17. FTIR ν/cm^{−1} (Nujol): 1949 (s), 1882 (w), 1819 (w), 1766 (w), 1658 (w), 1580 (s), 1304 (w), 1250 (s), 1182 (w), 1142 (w), 1069 (m), 1054 (m), 1032 (m), 1012 (m), 931 (s), 898 (s), 837 (s), 792 (m), 776 (m), 739 (m), 731 (m), 706 (s), 681 (w), 607 (m). μ_{eff} (Evans method, d₈-THF, 298 K): 2.10 μ_B.

Preparation of [U(Tren^{TMS})(THF)₂(μ-Cl)][BAR_f⁴] (8**).** THF (40 mL) was added to a cold (−78 °C) mixture of **5** (0.62 g, 0.73 mmol) and Et₃NH·BAR_f⁴ (0.70 g, 0.73 mmol). The resulting suspension was allowed to warm to ambient temperature while being stirred over 1 h, before being stirred at ambient temperature for a further 16 h. Volatiles were removed in vacuo to yield a yellow-brown oil that could not be purified. A solution of **1** (0.56 g, 0.73 mmol) in THF (10 mL) was then added, and the mixture allowed to stir for 16 h. Volatiles were removed in vacuo to afford a sticky brown-green solid. Toluene (40 mL) was added and briefly warmed to 60 °C, and the turbid mixture was allowed to cool to ambient temperature while stirring before being stirred at ambient temperature for a further 16 h. The brown suspension was allowed to settle before the solution was filtered away from the fine precipitate, reduced in volume to 1 mL and stored at −30 °C for 12 h to yield pale green crystals of **8** suitable for single-crystal X-ray crystallography. Yield: 0.61 g, 37%. Anal. Calcd for C₇₀H₁₀₆BClF₂₄N₈O₂Si₆U₂: C, 37.56; H, 4.77; N, 5.01%. Found: C, 37.25; H, 4.42; N, 4.73%. ¹H NMR: (C₆D₆, 298 K) δ −40.15 (s, 6H, CH₂), −27.45 (s, 6H CH₂), −25.80 (s, 6H CH₂), −19.91 (s, 6H CH₂), 0.22 (m, 27H, SiMe₃), 0.99 (m, 27H, SiMe₃), 4.60 (s, 8H, THF), 8.21 (m, 3H, Ar−H), 13.82 (s, br, 8H, THF). FTIR ν/cm^{−1} (Nujol): 3403 (w), 1609 (w), 1280 (s), 1260 (m), 1164 (m), 1130 (s), 1058 (w), 1018 (w), 984 (w), 929 (w), 919 (w), 889 (w), 839 (m), 772 (w), 744 (w), 719 (m), 682 (w). μ_{eff} (Evans method, 298 K): 3.51 μ_B.

Preparation of [U(Tren^{TMS})(THF)(μ-OC)Mn(CO)₄] (9**).** THF (30 mL) was added to a cold (−78 °C) mixture of **7** (1.15 g, 1.00 mmol) and K[Mn(CO)₅] (0.234 g, 1.00 mmol). The mixture was allowed to warm to room temperature and was stirred for 12 h. The mixture was allowed to settle (1 h), and the solution was filtered from the white precipitate. Volatiles were removed at reduced pressure, and the resulting yellow-brown solid was extracted into warm toluene (10 mL).

The volume of toluene was reduced to ~1 mL, and **9** crystallized as yellow blocks at $-30\text{ }^{\circ}\text{C}$ over a period of 48 h. Yield: 54%. Anal. Calcd for $\text{C}_{24}\text{H}_{47}\text{MnN}_4\text{O}_6\text{Si}_3\text{U}$: C, 33.33; H, 5.48; N, 6.48%. Found: C, 34.11; H, 5.67; N, 6.60%. $^1\text{H NMR}$ (C_6D_6 , 295 K): δ -42.25 (6H, s, br, CH_2), 3.53 (4H, s, THF), 5.73 (27H, s, SiMe_3), 15.65 (6H, d, br, CH_2), 33.90 (4H, s, THF). FTIR ν/cm^{-1} (Nujol): 1931 (s), 1918 (s), 1889 (s), 1709 (s), 1249 (m), 1082 (m), 1061 (m), 1018 (m), 928 (s), 907 (s), 836 (s), 775 (m), 718 (m), 675 (m). μ_{eff} (Evans method, C_6D_6 , 295 K): $2.94\ \mu_{\text{B}}$.

Preparation of $[\{\text{U}(\text{Tren}^{\text{TMS}})(\text{DME})\}[\text{Mn}(\text{CO})_5]$ (10**).** DME (30 mL) was added to a cold ($-78\text{ }^{\circ}\text{C}$) mixture of **7** (1.15 g, 1.00 mmol) and $\text{K}[\text{Mn}(\text{CO})_5]$ (0.234 g, 1.00 mmol). The clear green reaction mixture was heated to $\sim 75\text{ }^{\circ}\text{C}$ for 3 h, whereupon the color of the solution gradually changed from green to yellow-brown. The solution was allowed to cool to ambient temperature (1 h), and volatiles were removed in vacuo to yield a brown solid. Toluene (~30 mL) was added, and the resulting suspension was gently warmed to $\sim 60\text{ }^{\circ}\text{C}$ while stirring, before being allowed to settle and cool to ambient temperature (30 min). The yellow-brown solution was filtered away from the white precipitate, before the solvent was reduced in volume to 1 mL in vacuo and stored at $-30\text{ }^{\circ}\text{C}$ for 72 h to yield yellow crystals of **10**. Yield: 0.21 g, 24%. Anal. Calcd for $\text{C}_{24}\text{H}_{49}\text{MnN}_4\text{O}_7\text{Si}_3\text{U}$: C, 32.65; H, 5.59; N, 6.34%. Found: C, 31.84; H, 5.81; N, 8.62%. $^1\text{H NMR}$: (C_6D_6 , 298 K) δ -46.14 (s, 6H, CH_2); -40.41 (s, 2H, OCH_2); 6.47 (s, 6H, OMe); 12.61 (s, 27H SiMe_3); 13.21 (s, 6H, CH_2); 18.76 (s, 2H, OCH_2). FTIR ν/cm^{-1} (Nujol): 2726 (w), 2045 (m), 2013 (m), 1982 (w), 1971 (w), 1960 (w), 1939 (s), 1921 (s), 1892 (s), 1859 (s), 1840 (m), 1261 (s), 1248 (s), 1020 (m), 927 (m), 839 (s), 773 (w), 722 (m), 684 (m). μ_{eff} (Evans method, C_6D_6 , 298 K): $3.35\ \mu_{\text{B}}$.

Preparation of $[\{\text{U}(\text{Tren}^{\text{TMS}})(\mu\text{-OC})_2\text{Mn}(\text{CO})_3\}_2]$ (11**).** $[\text{Mn}(\text{CO})_5\text{H}]$ (0.20 g, 1.00 mmol) in toluene (10 mL) was added to a cold ($-78\text{ }^{\circ}\text{C}$) solution of **5** (0.78 g, 1.00 mmol) in toluene. The resulting solution was allowed to warm to ambient temperature while being stirred (1 h), before being stirred at ambient temperature for a further 16 h. Volatiles were removed in vacuo to yield a yellow-brown solid. Hexane (40 mL) was added, and the resulting suspension was gently warmed to $\sim 50\text{ }^{\circ}\text{C}$ while stirring, before being allowed to settle and cool to ambient temperature (30 min). The yellow-brown solution was filtered away from the small amount of precipitate, before the solvent was removed in vacuo. To the yellow-brown residue was added hexane (2 mL) and toluene (1.25 mL), the suspension was warmed to $60\text{ }^{\circ}\text{C}$, allowed to cool to ambient temperature, and stored at $-30\text{ }^{\circ}\text{C}$ for 18 h to yield yellow crystals of **11** suitable for single-crystal X-ray crystallography. Yield: 0.58 g (73%). Anal. Calcd for $\text{C}_{40}\text{H}_{78}\text{Mn}_2\text{N}_8\text{O}_{10}\text{Si}_6\text{U}_2$: C, 30.30; H, 4.96; N, 7.07%. Found: C, 30.16; H, 5.01; N, 5.17%. $^1\text{H NMR}$: (C_6D_6 , 298 K) δ -45.21 (s, 12H, CH_2); 11.03 (s, 54H, SiMe_3); 19.25 (s, 12H CH_2). FTIR ν/cm^{-1} (Nujol): 2361 (w), 2343 (w), 2062 (w), 2035 (m), 2014 (w), 1952 (s), 1938 (s), 1823 (s), 1814 (s), 1731 (s), 1590 (w), 1303 (w), 1260 (m), 1248 (m), 1180 (w), 1142 (w), 1074 (m), 1061 (m), 1020 (m), 928 (m), 903 (m), 870 (m), 834 (s), 772 (m), 747 (w), 723 (m), 682 (m), 669 (m), 617 (w), 589 (w), 571 (w), 547 (w). μ_{eff} (Evans method, C_6D_6 , 298 K): $3.93\ \mu_{\text{B}}$.

Preparation of $[\{\text{U}(\text{Tren}^{\text{DMSB}})(\mu\text{-OC})_2\text{Mn}(\text{CO})_3\}_2]$ (12**).** $[\text{Mn}(\text{CO})_5\text{H}]$ (0.20 g, 1.00 mmol) in toluene (10 mL) was added to a cold ($-78\text{ }^{\circ}\text{C}$) solution of **C** (0.72 g, 1.00 mmol) in toluene (10 mL). The resulting solution was allowed to warm to ambient temperature while being stirred (1 h), before being stirred at ambient temperature for a further 16 h. Volatiles were removed in vacuo to yield a yellow-green solid. To this was added toluene (~10 mL), the suspension was warmed to $\sim 60\text{ }^{\circ}\text{C}$, allowed to cool to ambient temperature, and stored at $-30\text{ }^{\circ}\text{C}$ for 18 h to yield yellow-green crystals of **12** suitable for single-crystal X-ray crystallography. Yield: 0.55 g (60%). Anal. Calcd for $\text{C}_{29}\text{H}_{57}\text{MnN}_4\text{O}_5\text{Si}_3\text{U}$: C, 37.89; H, 6.26; N, 6.10%. Found: C, 37.87; H, 6.17; N, 6.36%. $^1\text{H NMR}$: (C_6D_6 , 298 K) δ -38.24 (s, 12H, CH_2); 7.75 (s, 36H, SiMe_2); 9.38 (s, 54H, ^tBu); 15.45 (s, 12H, CH_2). FTIR

ν/cm^{-1} (Nujol): 2730 (w), 1956 (s), 1806 (s), 1734 (s), 1614 (w), 1259 (m), 1250 (m), 1078 (m), 1030 (m), 936 (w), 828 (m), 802 (m), 776 (m), 744 (w), 712 (w), 696 (w), 679 (m), 669 (m), 565 (w), 549 (m), 455 (m). μ_{eff} (Evans method, C_6D_6 , 298 K): $4.09\ \mu_{\text{B}}$.

Preparation of $[\{\text{U}(\text{Tren}^{\text{TMS}})_2(\mu\text{-O})]$ (13**).** THF (~30 mL) was added to a cold ($-78\text{ }^{\circ}\text{C}$) mixture of **7** (1.15 g, 1.00 mmol) and $\text{K}[\text{Mn}(\text{Cp})_2]$ (0.16 g, 1.00 mmol). The mixture was allowed to warm to room temperature and was stirred for 12 h. The mixture was allowed to settle (1 h), and the solution was filtered from the off-white precipitate. Volatiles were removed at reduced pressure, and the resulting red-brown solid was extracted into warm toluene (10 mL). The volume of toluene was reduced to ~1 mL, and **13** crystallized as yellow plates at $-30\text{ }^{\circ}\text{C}$ over a period of 48 h. Yield: 0.99 g, 82%. Anal. Calcd for $\text{C}_{30}\text{H}_{78}\text{N}_8\text{O}\text{Si}_6\text{U}_2$: C, 29.74; H, 6.49; N, 9.25%. Found: C, 30.96; H, 6.50; N, 9.10%. $^1\text{H NMR}$ (C_6D_6 , 295 K): δ -25.59 (12H, s, CH_2), -23.25 (54H, s, SiMe_3), 76.40 (12H, s, CH_2). FTIR ν/cm^{-1} (Nujol): 1605 (w), 1550 (w), 1330 (m), 1247 (s), 1069 (s), 1059 (s), 926 (s), 893 (m), 771 (s), 721 (s), 685 (w), 673 (w), 548 (s), 432 (m), 412 (m). μ_{eff} (Evans method, C_6D_6 , 295 K): $2.95\ \mu_{\text{B}}$.

X-ray Crystallography. Crystal data for compounds **2–13** are given in the Supporting Information. Bond lengths are listed in Tables 1, 3, and 5. Crystals were examined variously on Bruker AXS SMART 1000 or SMART APEX CCD area detector diffractometers using graphite-monochromated $\text{MoK}\alpha$ radiation ($\lambda = 0.71073\text{ \AA}$). Intensities were integrated from a sphere of data recorded on narrow (0.3°) frames by ω rotation. Cell parameters were refined from the observed positions of all strong reflections in each data set. Semiempirical absorption corrections based on symmetry-equivalent and repeat reflections were applied. The structures were solved by direct methods and were refined by full-matrix least-squares on all unique F^2 values, with anisotropic displacement parameters for all non-hydrogen atoms, and with constrained riding hydrogen geometries; $U_{\text{iso}}(\text{H})$ was set at 1.2 (1.5 for methyl groups) times U_{eq} of the parent atom. The largest features in final difference syntheses were close to heavy atoms and were of no chemical significance. Highly disordered solvent molecules of crystallization in $5\cdot 2\text{C}_7\text{H}_8$, could not be modeled and were treated with the PLATON SQUEEZE procedure.^{55,56} Programs were Bruker AXS SMART (control) and SAINT (integration),⁵⁷ and SHELXTL was employed for structure solution and refinement and for molecular graphics.⁵⁸

■ ASSOCIATED CONTENT

S Supporting Information. Crystallographic details for **2–13**. This material is available free of charge via the Internet at <http://pubs.acs.org>.

■ AUTHOR INFORMATION

Corresponding Author

*E-mail: stephen.liddle@nottingham.ac.uk.

■ ACKNOWLEDGMENT

We thank the Royal Society for a University Research Fellowship (S.T.L.), the EPSRC, ERC, University of Nottingham, and the U.K. National Nuclear Laboratory for generously supporting this work, and Mr. A. J. Wooles (University of Nottingham) for obtaining the FTIR spectra of $\text{K}[\text{Mn}(\text{CO})_5]$ and $[\text{HMn}(\text{CO})_5]$ in Nujol.

■ REFERENCES

- (1) Ephritikhine, M. *Dalton Trans.* **2006**, 2501.

- (2) Sessler, J. L.; Melfi, P. J.; Pantos, G. D. *Coord. Chem. Rev.* **2006**, *250*, 816.
- (3) Evans, W. J.; Kozimor, S. A. *Coord. Chem. Rev.* **2006**, *250*, 911.
- (4) Lam, O. P.; Anthon, C.; Meyer, K. *Dalton Trans.* **2009**, 9677.
- (5) Graves, C. R.; Kiplinger, J. L. *Chem. Commun.* **2009**, 3831.
- (6) Liddle, S. T.; Mills, D. P. *Dalton Trans.* **2009**, 5592.
- (7) Liddle, S. T. *Phil. Trans. R. Soc. A.* **2009**, *465*, 1673.
- (8) Moris, E.; Eisen, S. *Coord. Chem. Rev.* **2006**, *250*, 855.
- (9) Castro-Rodríguez, I.; Meyer, K. *Chem. Commun.* **2006**, 1353.
- (10) Berthet, J. C.; Ephritikhine, M. *Coord. Chem. Rev.* **1998**, *178–180*, 83.
- (11) Hayton, T. W. *Dalton Trans.* **2010**, *39*, 1145.
- (12) Fox, A.; Bart, S. C.; Meyer, K.; Cummins, C. C. *Nature* **2008**, *455*, 341.
- (13) Pyykkö, P.; Atsumi, M. *Chem.—Eur. J.* **2009**, *15*, 186.
- (14) Scott, P.; Hitchcock, P. B. *Polyhedron* **1994**, *13*, 1651.
- (15) Scott, P.; Hitchcock, P. B. *J. Chem. Soc., Dalton Trans.* **1995**, 603.
- (16) Roussel, P.; Hitchcock, P. B.; Tinker, N.; Scott, P. *Chem. Commun.* **1996**, 2053.
- (17) Roussel, P.; Hitchcock, P. B.; Tinker, N. D.; Scott, P. *Inorg. Chem.* **1997**, *36*, 5716.
- (18) Kaltsoyannis, N.; Scott, P. *Chem. Commun.* **1998**, 1665.
- (19) Roussel, P.; Scott, P. *J. Am. Chem. Soc.* **1998**, *120*, 1070.
- (20) Boaretto, R.; Roussel, P.; Alcock, N. W.; Kingsley, A. J.; Munslow, I. J.; Sanders, C. J.; Scott, P. *J. Organomet. Chem.* **1999**, *591*, 174.
- (21) Boaretto, R.; Roussel, P.; Kingsley, A. J.; Munslow, I. J.; Sanders, C. J.; Alcock, N. W.; Scott, P. *Chem. Commun.* **1999**, 1701.
- (22) Roussel, P.; Alcock, N. W.; Boaretto, R.; Kingsley, A. J.; Munslow, I. J.; Sanders, C. J.; Scott, P. *Inorg. Chem.* **1999**, *38*, 3651.
- (23) Roussel, P.; Errington, W.; Kaltsoyannis, N.; Scott, P. *J. Organomet. Chem.* **2001**, *635*, 69.
- (24) Roussel, P.; Boaretto, R.; Kingsley, A. J.; Alcock, N. W.; Scott, P. *J. Chem. Soc., Dalton Trans.* **2002**, 1423.
- (25) Duval, P. B.; Burns, C. J.; Buschmann, W. E.; Clark, D. L.; Morris, D. E.; Scott, B. L. *Inorg. Chem.* **2001**, *40*, 5491.
- (26) Newell, B. S.; Rappé, A. K.; Shores, M. P. *Inorg. Chem.* **2010**, *49*, 1595.
- (27) Liddle, S. T.; McMaster, J.; Mills, D. P.; Blake, A. J.; Jones, C.; Woodul, W. D. *Angew. Chem., Int. Ed.* **2009**, *48*, 1077.
- (28) Liddle, S. T.; Mills, D. P.; Gardner, B. M.; McMaster, J.; Jones, C.; Woodul, W. D. *Inorg. Chem.* **2010**, *48*, 3520.
- (29) Gardner, B. M.; McMaster, J.; Lewis, W.; Liddle, S. T. *Chem. Commun.* **2009**, 2851.
- (30) Gardner, B. M.; McMaster, J.; Lewis, W.; Blake, A. J.; Liddle, S. T. *J. Am. Chem. Soc.* **2009**, *131*, 10388.
- (31) Patel, D.; Lewis, W.; Blake, A. J.; Liddle, S. T. *Dalton Trans.* **2010**, *39*, 6638.
- (32) Liddle, S. T.; Gardner, B. M. *J. Organomet. Chem.* **2009**, *694*, 1581.
- (33) Patel, D.; King, D. M.; Gardner, B. M.; McMaster, J.; Lewis, W.; Blake, A. J.; Liddle, S. T. *Chem. Commun.* **2011**, *47*, 295.
- (34) Gardner, B. M.; McMaster, J.; Moro, F.; Lewis, W.; Blake, A. J.; Liddle, S. T. *Chem.—Eur. J.* **2011**, *17*, 6909.
- (35) An analogous alkane-elimination strategy afforded a yttrium-rhenium bond, see Butovskii, M. V.; Tok, O. L.; Wagner, F. R.; Kempe, R. *Angew. Chem., Int. Ed.* **2008**, *47*, 6469.
- (36) For example, the use of borate anions enables access to tris-Cp* rare earth and actinide complexes, see Evans, W. J. *Inorg. Chem.* **2007**, *46*, 3435.
- (37) For example, a previous attempt by Porchia to prepare a uranium–silicon bond in THF resulted in formation of the corresponding siloxide by oxo-abstraction from the THF, see Porchia, M.; Brianese, N.; Casellato, U.; Ossola, F.; Rossetto, G.; Zanella, P.; Graziani, R. *J. Chem. Soc., Dalton Trans.* **1989**, 677.
- (38) Maynadié, J.; Berthet, J.-C.; Thuéry, P.; Ephritikhine, M. *Organometallics* **2006**, *25*, 5603.
- (39) As evidenced from a search of the Cambridge Structural Database (CSD version 1.11, date: 29/05/2011): (a) Allen, F. H. *Acta Crystallogr., Sect. B* **2002**, *58*, 380. (b) Allen, F. H.; Kennard, O. *Chem. Des. Autom. News* **1993**, *8*, 31.
- (40) Cotton, S. In *Lanthanide and Actinide Chemistry*; Wiley: Chichester, U.K., 2006.
- (41) Evans, W. J.; Kozimor, S. A.; Ziller, J. W. *Chem. Commun.* **2005**, 4681.
- (42) Evans, W. J.; Nyce, G. W.; Forrestal, K. J.; Ziller, J. W. *Organometallics* **2002**, *21*, 1050.
- (43) Evans, W. J.; Miller, K. A.; Hillman, W. R.; Ziller, J. W. *J. Organomet. Chem.* **2007**, *692*, 3649.
- (44) Amorose, D. M.; Lee, R. A.; Petersen, J. L. *Organometallics* **1991**, *10*, 2191.
- (45) Reger, D. L.; Wright, T. D.; Little, C. A.; Lamba, J. J. S.; Smith, M. D. *Inorg. Chem.* **2001**, *40*, 3810.
- (46) Lukehart, C. M.; Torrence, G. P.; Zeile, J. V. *Inorg. Synth.* **1991**, *28*, 199.
- (47) Nappa, M. J.; Santi, R.; Halpern, J. *Organometallics* **1985**, *4*, 34.
- (48) Tilley, T. D.; Andersen, R. A. *J. Chem. Soc., Chem. Commun.* **1981**, 985.
- (49) Selent, D.; Ramm, M.; Janiak, C. *J. Organomet. Chem.* **1995**, *501*, 235.
- (50) Boncella, J. M.; Andersen, R. A. *Inorg. Chem.* **1984**, *23*, 432.
- (51) Robbins, J. L.; Edelstein, N. M.; Cooper, S. R.; Smart, J. C. *J. Am. Chem. Soc.* **1979**, *101*, 3853.
- (52) Elschenbroich, C. *Organometallics*, 3rd ed.; Wiley-VCH: Weinheim, Germany, 2005; pp 513.
- (53) Oxo-group abstraction from THF has been observed during attempts to prepare a U–Sn bond resulting in a U–O–Sn linkage, see Porchia, M.; Casellato, U.; Ossola, F.; Rossetto, G.; Zanella, P.; Graziani, R. *Chem. Commun.* **1986**, 1034.
- (54) Barker, B. J.; Sears, P. G. *J. Phys. Chem.* **1974**, *78*, 2687.
- (55) Sluis, P. v. d.; Spek, A. L. *Acta Crystallogr., Sect. A* **1990**, *46*, 194.
- (56) Spek, A. L. *Acta Crystallogr., Sect. D* **2009**, *65*, 148.
- (57) Bruker SMART and SAINT; Bruker AXS Inc.: Madison, Wisconsin, 2001.
- (58) Sheldrick, G. M. *Acta Crystallogr., Sect. A* **2008**, *64*, 112.